

Point Could Mamba: Point Cloud Learning via State Space Model

Tao Zhang^{1,2*}, Xiangtai Li², Haobo Yuan¹, Shuping Ji¹, Shuicheng Yan²

¹Wuhan University ²Skywork AI

<https://github.com/zhang-tao-whu/PCM>

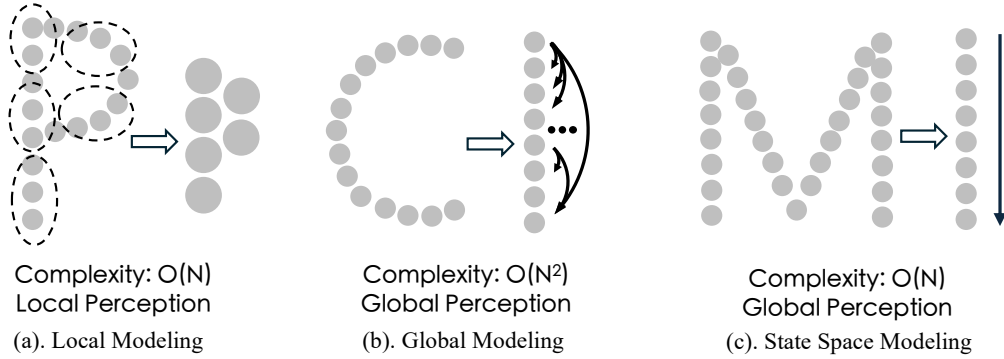


Figure 1: Several pipelines of point cloud modeling. (a) denotes point-based methods, including point-based methods, such as PointNet [32], PointNet++ [33], PointMLP [28], and PointNeXt [35]. (b) is transformer-based methods, including Point Transformer [61] and Point-MAE [30]. (c) represents Mamba-based methods, which offer advantages of global modeling and linear computational complexity.

Abstract

In this work, for the first time, we demonstrate that Mamba-based point cloud methods can outperform point-based methods. Mamba exhibits strong global modeling capabilities and linear computational complexity, making it highly attractive for point cloud analysis. To enable more effective processing of 3-D point cloud data by Mamba, we propose a novel Consistent Traverse Serialization to convert point clouds into 1-D point sequences while ensuring that neighbouring points in the sequence are also spatially adjacent. Consistent Traverse Serialization yields six variants by permuting the order of x, y, and z coordinates, and the synergistic use of these variants aids Mamba in comprehensively observing point cloud data. Furthermore, to assist Mamba in handling point sequences with different orders more effectively, we introduce point prompts to inform Mamba of the sequence's arrangement rules. Finally, we propose positional encoding based on spatial coordinate mapping to inject positional information into point cloud sequences better. Based on these improvements, we construct a point cloud network named Point Cloud Mamba, which combines local and global modeling. Point Cloud Mamba surpasses the SOTA point-based method PointNeXt and achieves new SOTA performance on the ScanObjectNN, ModelNet40, and ShapeNetPart datasets.

1 Introduction

Point cloud analysis has become a popular topic in understanding 3D and has drawn attention from the research community. Unlike 2D image processing, point clouds are composed of unordered

*This work was performed when Tao Zhang was an Intern at Skywork AI.

and irregular point sets, which makes it hard to apply the 2D image processing methods directly. Thus, recent deep-learning-based approaches have various representations, such as voxel-based and point-based methods. The representative works, Point-Net and Point-Net++, adopt the MLP-based design with deep hierarchical local priors, shown in Fig. 1 (a). After that, many research works focus on advanced local geometric modeling via convolution, graph modeling, or attention.

Meanwhile, with the rapid progress of vision transformers, several works enhance the global modeling with transformer structure in point could, as shown in Fig. 1 (b). In addition, transformer architectures also work effectively in mask point pre-training, 3D segmentation, and in-context learning. However, the computation and memory costs are still huge. Recently, state space models [8, 10] (SSMs) have been proven to model long-range dependency in sequential data. In particular, Mamba [8] is proven effective as Transformer [44] for several challenging NLP tasks. After that, recent works explore SSMs in various vision tasks, including image representation learning, medical segmentation, and low-level vision tasks. One concurrent work, PointMamba, directly uses the Mamab layer to model the global context. However, there are still significant performance gaps between PointMamba and previous point-based methods.

In this work, we ask an essential question: Can we achieve an efficient point cloud analysis architecture using Mamba and surpass the performance of point-based methods? In particular, we introduce the Point Cloud Mamba (PCM), a combining local and global modelling framework that outperforms the SOTA point-based method PointNeXt [35].

PCM utilizes Mamba to model the global features of point clouds while maintaining linear computational complexity. To process 3-D point cloud data effectively by Mamba layers, we propose Consistent Traverse Serialization (CTS) to serialize point clouds into a 1-D point sequence while ensuring that neighbouring points in the sequence are also adjacent in space. Then, CTS can easily derive six variants by simply permuting the order of x, y, and z coordinates. Surprisingly, when these six variants of CTS are combined, Mamba layers can more effectively model point cloud features because different variants provide different perspectives of the point cloud. To facilitate Mamba in handling specific point sequences better, we introduce order prompts to provide Mamba with the arrangement rules of the current point sequence. Finally, we propose simple spatial coordinate mapping as positional embedding for points, more suitable for irregular point cloud data than RoPE [40] and learnable embedding.

Thanks to the improvements above, we successfully introduced Mamba into Point Cloud analysis and obtained Point Cloud Mamba (PCM). PCM outperforms the SOTA point-based method PointNeXt on three datasets: ScanObjectNet [43], ModelNet40 [50], and ShapeNetPart [58]. On the ShapeNetPart part segmentation dataset, PCM-Tiny surpasses PointNeXt with a 0.4 OA improvement, using only 39% of the parameter of PointNeXt.

In summary, we have the following contributions in this work: 1) We introduce Mamba into point cloud analysis and construct a combined local and global modeling framework named Point Cloud Mamba. 2) We propose consistent traverse serialization, order prompts, and positional encoding based on spatial coordinate mapping to assist Mamba in better handling point cloud data. 3) Point Cloud Mamba is the first Mamba-based method that works well in point cloud analysis. It outperforms the SOTA point-based method PointNeXt on ScanObjectNet, ModelNet40, and ShapeNetPart datasets.

2 Related Work

3D Point Clouds Classification. Recent works have used deep neural networks to process 3D point clouds. In particular, representative works, PointNet [32] and PointNet++ [33], are the pioneering point-based approaches to directly handle the point clouds using MLPs. Meanwhile, several works explore graph-based modeling to utilize 3D geometric topology. Then, several works [47, 42, 39, 21, 55, 15] explore the local geometric features via different kernel modeling. Moreover, several works [24, 56, 51, 36, 4, 14, 23, 53, 60, 28] explore other point cloud architecture designs, including MLPs and transformers. Several works also explore different pre-training methods [31, 59] or in-context abilities [6, 45] inspired by the NLP field. Recently, state space models [10, 8] have achieved significant progress. Compared with transformers, they have advantages in efficient global modeling. A concurrent work [22] explores such architecture in point clouds. However, there are still significant performance gaps, compared with previous point cloud methods. For the first time, our work shows

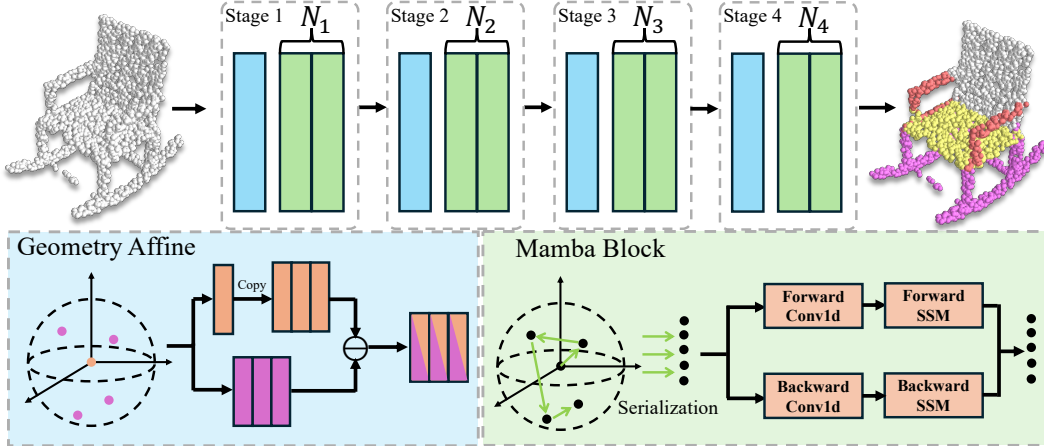


Figure 2: **The architecture of our proposed Point Cloud Mamba.** PCM consists of four stages, each comprising a geometric affine module and several mamba layers. Point downsampling is performed between stages.

that Mamba architecture can achieve comparable or even better results than transformer-based models in 3D point clouds.

3D Visual Transformers. With the rise of the transformer in 2D version [5, 20, 2], several works [16, 11, 38, 41, 17] also explore transformer architectures in the point cloud. Earlier works [11, 61] have focused on the point cloud process. PCT [11] performs global attention directly to each point, following the ViT [5]. However, it has memory consumption and computational complexity issues. Point Transformer [61] solves this issue by introducing local attention. Then, the updated versions [49, 48] explore the different architectures to improve performance and efficiency. Inspired by these studies, our works combine local point processing and a new traverse serialization strategy, which leads to better results than direct SSM traverse.

State Space Models. Inspired by continuous state space models in control systems, recently, state space models [8, 10] have been proven to model long-range dependency. In particular, S4 [10] proposes to normalize the parameter into the diagonal structure, which results in less computation cost and memory usage. After that, Mamba [8] presents a selection mechanism that leads to better results than transformers. Recently, several works have explored such architecture in different tasks, including image classification [62, 25, 19], graph modeling [1], medical segmentation [27, 54, 57, 37], and low-level version tasks [12]. As a concurrent work, we further prove the potential of SSMs in the 3D point clouds, where we can achieve even better results than previous architectures.

3 Method

The SSM-based architecture, Mamba [8], is attractive for point cloud representation learning due to its global modeling capability and linear computational complexity. However, Mamba is designed for the causal modeling of 1-D sequences, making it difficult to directly apply it to the modeling of non-causal 3-D point cloud data, posing many challenges to be addressed.

This section explores how to effectively integrate Mamba into architectures based on local modeling to capture global features. We first review PointMLP [28], a straightforward local modeling architecture, in Sec. 3.1, and then review Mamba, a global modeling architecture with linear complexity, in Sec. 3.2. Next, in Sec. 3.3, we introduce how to combine Mamba with PointMLP to obtain a point cloud network based on Mamba architecture. Finally, we introduce improving this naive Mamba-based network to Point Cloud Mamba in Sec. 3.4. We propose consistent traverse serialization, order prompt, new positional embedding, and more reasonable architectures to assist Mamba in modelling point cloud data better.

3.1 PointMLP Formulation

PointMLP [28] models the representation of point clouds using simple MLP and expands the receptive field of each point through point cloud downsampling and local feature aggregation. The process can be described by Equation 1 and 2:

$$f_i^{l+1} = \Phi_{pos}(\mathcal{A}(\Phi_{pre}(GAM(\{f_{i,j}^l\})), |j=1, \dots, K)), \quad (1)$$

$$GAM(\{f_{i,j}^l\}) = \alpha \odot \frac{\{f_{i,j}^l\} - f_i^l}{\sigma + \delta}, \quad \sigma = \sqrt{\frac{1}{k \times n \times d} \sum_{i=1}^n \sum_{j=1}^k (f_{i,j}^l - f_i^l)^2}, \quad (2)$$

where Φ represents a network composed of a series of residual MLPs, $\{f_{i,j}^l | j = 1, \dots, k\}$ represents the K neighboring points of f_i^l , \mathcal{A} denotes the max-pooling operation. GAM refers to the Geometric Affine Module proposed by PointMLP to enhance local features.

PointMLP enhances the features of point clouds by iteratively performing the above process and downsampling the point cloud between different stages to expand the receptive field. However, even though the GAM combined with the point cloud downsampling strategy can expand the receptive field of the point cloud, PointMLP still struggles to extend the receptive field to the entire global point cloud, thus lacking in global modeling of the point cloud.

3.2 Mamba Formulation

The state-space equation can describe a multi-input, multi-output continuous system where the current inputs and states jointly determine the change in the state space of this system:

$$\dot{h}(t) = \mathbf{A}h(t) + \mathbf{B}x(t), \quad y(t) = \mathbf{C}h(t), \quad (3)$$

where $x(t)$, $h(t)$, and $y(t)$ are the inputs, states, and outputs of the current system, respectively. \mathbf{A} , \mathbf{B} , and \mathbf{C} are all continuous parameters of the system.

The continuous state-space equation mentioned above can be transformed into a discrete formulation using a timescale parameter Δ based on the zero-order hold rule:

$$\bar{\mathbf{A}} = \exp(\Delta \mathbf{A}), \quad \bar{\mathbf{B}} = (\Delta \mathbf{A})^{-1}(\exp(\Delta \mathbf{A}) - I) \cdot \Delta \mathbf{B}, \quad (4)$$

$$h_t = \bar{\mathbf{A}}h_{t-1} + \bar{\mathbf{B}}x_t, \quad y_t = \mathbf{C}h_t, \quad (5)$$

where x_t , h_t , and y_t are the system's discrete inputs, states, and outputs. $\bar{\mathbf{A}}$, $\bar{\mathbf{B}}$ are all discrete parameters of the system.

Inspired by equations 4 and 5, some SSM-based models have been proposed and demonstrated superiority in long sequence modeling. However, early SSM-based methods like S4 [9] assume linear time invariance (LTI), which limits their modeling capabilities. Recently, Mamba [8], a new SSM-based model that introduces time-varying system parameters, has been introduced. Specifically, Δ , $\bar{\mathbf{A}}$, and $\bar{\mathbf{B}}$ are all functions of x_t . Mamba demonstrates long sequence modeling capabilities comparable to Transformer and achieves linear computational complexity during inference following equation 5.

However, equation 5 is difficult to compute in parallel. It can be expanded and implemented using global convolution to enhance the efficiency of training Mamba on GPUs:

$$\bar{\mathbf{K}} = (\mathbf{C}\bar{\mathbf{B}}, \mathbf{C}\bar{\mathbf{A}}\bar{\mathbf{B}}, \dots, \mathbf{C}\bar{\mathbf{A}}^{M-1}\bar{\mathbf{B}}), \quad y = x * \bar{\mathbf{K}}, \quad (6)$$

where M is the length of the input sequence x , and $\bar{\mathbf{K}}$ is the kernel of the global convolution.

3.3 A Naive Mamba-based Point Cloud Network

Using Mamba [8] to replace the MLP operator in PointMLP [28] to achieve global modeling capabilities is a natural idea. However, this still requires addressing two challenges: 1) Point clouds are 3-D data, so how can we transform them into 1-D sequences? 2) Mamba is designed for causal modeling, so how can Mamba handle non-causal point cloud data? To address these challenges, we first adopt the z-order [29] serialization method to flatten 3-D point cloud data into 1-D sequences,

allowing point cloud data to be processed by Mamba. Secondly, inspired by [62] and [25], we use bidirectional Mamba to allow each point to obtain features from any other point. At this point, we have implemented a naive Mamba-based network for the point cloud:

$$f_i^{l+1} = \text{Mamba}(x^l, \text{reverse}(x^l)), \quad x^l = \mathcal{S}_z(\mathcal{A}(\text{GAM}(\{f_{i,j}^l | j = 1, \dots, k\}))) \quad (7)$$

where \mathcal{S}_z refers to serialization according to the z-order.

3.4 Point Cloud Mamba

In Sec. 3.3, we obtained a naive mamba-based point cloud network; however, there is still plenty of room for optimization. Next, we will elaborate on improving this naive architecture to Point Cloud Mamba (PCM) and achieving performance beyond PointNeXt [35].

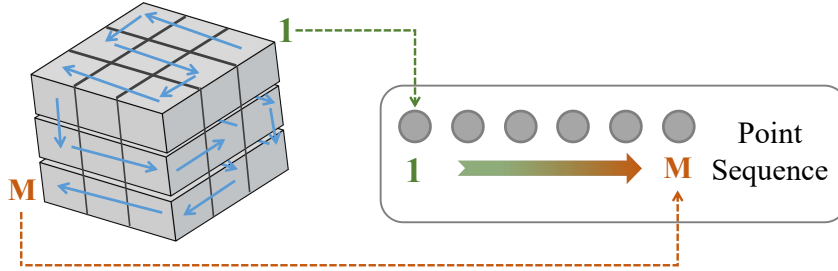


Figure 3: **The consistent traverse serialization strategy.** The 3-D point cloud data is voxelized and then serialized into a 1-D point sequence according to a predefined order. M represents the total number of points in the point cloud. With the permutation of x, y, and z coordinates, consistent traverse serialization has six variants.

Serialization strategy. How to convert 3-D point cloud data into a 1-D sequence that Mamba can handle is crucial. We find that point cloud sequences arranged according to specific rules can be better processed by Mamba compared to disordered point cloud sequences. For example, randomly flattening point cloud data into a 1-D point sequence and feeding it into Mamba for modelling will significantly underperform compared to using an ordered point sequence (84.1 vs 86.7). Based on this, we propose the Consistent Traverse Serialization (CTS) strategy, which ensures that adjacent points in the sequence are also adjacent in spatial position. Figure 3 illustrates how CTS converts 3-D point clouds into a 1-D sequence.

Firstly, the point cloud is grid sampled to transform continuous spatial coordinates into discrete grid coordinates:

$$\{c_1^g, c_2^g, c_3^g\} = \text{int}(\{c_1^s, c_2^s, c_3^s\} \times N) \quad (8)$$

where $\{c_1^s, c_2^s, c_3^s\}$ and $\{c_1^g, c_2^g, c_3^g\}$ are the spatial and grid coordinates of the points, and N is the grid numbers. We design an encoding function that, given the coordinates of two dimensions, maps the coordinates to a code. Sorting the sequence according to the code ensures that adjacent points are contiguous in space.

$$\text{Code_func}(n_1, n_2) = \begin{cases} n_2 * N + n_1, & n_2 \% 2 = 0 \\ (n_2 + 1) * N - n_1, & n_2 \% 2 \neq 0 \end{cases} \quad (9)$$

Then, we can compute a code for each point based on its grid coordinates:

$$\text{code} = \text{Code_func}(\text{Code_func}(c_1^g, c_2^g), c_3^g). \quad (10)$$

Sorting the point cloud according to the **code** allows it to be flattened into a 1-D sequence. This simple serialization strategy performs comparably to carefully designed z-order [29] and Hilbert-order [13] serialization strategies. Additionally, by exchanging the order of the x, y, and z axes, six different serialization methods can be derived, which we call "xyz", "xzy", "yxz", "yzx", "zxy", and "zyx". These different serialization methods can be viewed as various point cloud observations from different spatial perspectives.

Additionally, combining multiple serialization strategies can effectively assist Mamba in better modeling point cloud features, as shown in Table 7. Specifically, we adopt different serialization

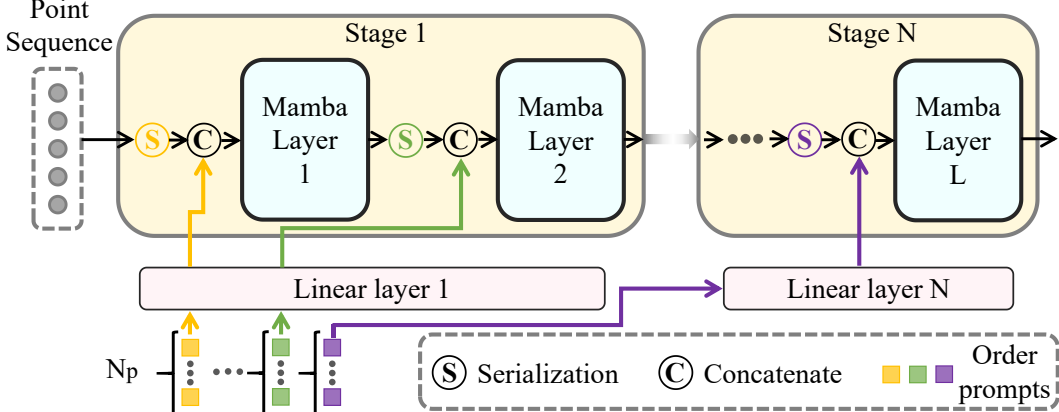


Figure 4: **The order prompts.** Different colors represent different serialization orders. N_p order prompts are mapped to the same channel size as the features and then concatenated to the beginning and end of the point sequence input to the mamba layer.

Table 1: **Architecture settings.** The parameters of the four stages are enclosed in curly braces { }, while the parameters corresponding to each Mamba layer within a stage are enclosed in square brackets [].

Architecture	Mamba layers	Serialization	Channels	Order Prompts
PCM-Tiny	{1, 1, 2, 2}	{[xyz]-[xzy]-[yxz, yzx]-[zxy-zyx]}	{192, 192, 384, 384}	6
PCM	{1, 2, 2, 4}	{[xyz]-[xzy, yzx]-[yzx, zxy]-[zxy, hilbert, z, z-trans]}	{384, 384, 768, 768}	6

strategies for the inputs of different Mamba layers, allowing Mamba to perceive the point cloud more comprehensively, thus significantly surpassing a single serialization strategy alone.

Order prompt. When multiple serialization strategies are combined, assigning an identifier to each serialization is necessary. The identifier can help the Mamba layers recognize the arrangement of point cloud sequences and better capture point cloud features. We propose a simple but efficient order prompt mechanism to achieve this goal, which resembles the system messages in large language models.

As shown in Figure 4, we assigned N_p learnable embeddings as order prompts for each serialization order. Before being processed by the Mamba layer, the point cloud sequence has the corresponding order prompts added to both the beginning and end of the sequence. Considering that the input feature dimensions of the Mamba layers at different stages may vary, we also allocate a shared Linear layer for all Mamba layers within each stage to map the order prompts to the required channel size.

Positional embedding. In sequence modeling, positional encoding is crucial and widely applied in text and image patch sequence modeling. For example, RoPE [40] and learnable positional embedding are widely used in text sequence modeling and image patch sequence modeling, respectively. However, we find that these positional encoding methods are unsuitable for point clouds due to the sparsity and irregular shapes. The spatial distances between any two adjacent points in a point cloud sequence vary significantly, making it difficult to use the sequence positional information to represent the spatial gaps between adjacent points accurately. We employ a shared positional mapping function to address this challenge to map the point spatial coordinates to positional embeddings with the same channel size as the features.

$$Emd_{pos} = \text{Linear}(\{c_1^s, c_2^s, c_3^s\}) \quad (11)$$

Emd_{pos} refers to the positional embedding projected from the spatial coordinates of the point. This simple positional mapping function accurately encodes the spatial information of points into features, and the positional embeddings corresponding to adjacent points in the sequence are similarly similar. Since the channel size of features varies across different stages of the network, we need to learn a private positional embedding function for each stage, and different Mamba layers within the same stage share the same positional encoding function.

Table 2: **3D object classification in ScanObjectNN and ModelNet40.** Averaged results in three random runs using 1024 points as input without normalization and voting are reported.

Method	ScanObjectNN (PB_T50_RS)		ModelNet40		Params. M
	OA (%)	mAcc (%)	OA (%)	mAcc (%)	
PointNet [32]	68.2	63.4	89.2	86.2	3.5
PointCNN [21]	78.5	75.1	92.2	88.1	0.6
DGCNN [46]	78.1	73.6	92.9	90.2	1.8
DeepGCN [18]	-	-	93.6	90.9	2.2
KPConv [42]	-	-	92.9	-	14.3
ASSANet-L [34]	-	-	92.9	-	118.4
SimpleView [7]	80.5±0.3	-	93.0±0.4	90.5±0.8	0.8
CurveNet [52]	-	-	93.8	-	2.0
PointMLP [28]	85.4±1.3	83.9±1.5	94.1	91.3	13.2
PointNet++ [33]	77.9	75.4	91.9	-	1.5
PointNeXt [35]	87.7±0.4	85.8±0.6	93.2±0.1	90.8±0.2	1.4
Transformer-based					
Point Cloud Transformer [11]	-	-	93.2	-	2.9
Point-BERT [59]	83.1	-	93.2	-	22.1
Point-MAE [30]	85.2	-	93.8	-	22.1
Mamba-based					
PointMamba [22]	84.9	-	-	-	12.3
PCM-Tiny (ours)	86.9±0.4	85.0±0.3	93.1±0.1	90.6±0.3	6.9
PCM (ours)	88.1 ±0.3	86.6 ±0.2	93.4±0.2	90.7±0.6	34.2

Architecture settings. Our network architecture comprises four stages, each containing a geometric affine module and several Mamba layers. The number of Mamba layers, serialization strategies, channel sizes, and order prompt counts in each stage of PCM-Tiny are illustrated in Table 1. Furthermore, we achieve PCM by increasing the number of Mamba layers and channel sizes and adopting new serialization methods accordingly.

4 Experiments

4.1 Experiment Setup

Detailed settings. We conduct experiments on three datasets: ScanObjectNN [43] classification, ModelNet40 [50] classification, and ShapeNetPart [3] part segmentation. We train PCM using the AdamW optimizer [26] with an initial learning rate of 1e-4, employing Cosine Decay and a weight decay of 1e-4. We perform warmup for 5 epochs and use a batch size of 32, consistent across all tasks unless otherwise specified. We train PCM for 250 epochs on the ScanObjectNN and ModelNet40 datasets and for 300 epochs on ShapeNetPart. For ScanObjectNN and ModelNet40, we followed the PointNeXt using 1024 points, randomly sampled during training, and using farthest point sampling during testing. For ShapeNetPart, 2,048 randomly sampled points with normals were used as input for training and testing. Following PointNeXt [35], PCM employs multi-step learning rate decay during training on ShapeNetPart, decaying at epochs 210 and 270, with a decay rate of 0.5. The experimental settings for PCM-Tiny are identical to PCM on all datasets. All ablation experiments are conducted using PCM as the default architecture, implemented on the ScanObjectNN dataset with training shortened to 125 epochs. Apart from this adjustment, all other settings are identical to the main experiment.

4.2 Main Results

3D object classification in ScanObjectNN dataset. ScanObjectNet [43] is a challenging point cloud classification dataset containing 15,000 real scanned objects categorized into 13 classes. It is known for its noise and occlusion challenges. Following PointMLP [28] and PointNeXt [35], we conducted experiments on PB_T50_RS, the most challenging and commonly used ScanObjectNN variant. As shown in Table 2, PCM achieved an OA of 88.1 and a mAcc of 86.6 on ScanObjectNN, surpassing

Table 3: **Part segmentation in ShapeNetPart.** \dagger denotes using voting by averaging the results of 10 randomly scaled input point clouds.

Method	ins. mIoU	cls. mIoU	Params.
PointNet [32]	83.7	80.4	3.6
DGCNN [46]	85.2	82.3	1.3
KPConv [42]	86.4	85.1	-
CurveNet [52]	86.8	-	-
ASSANet-L [34]	86.1	-	-
Point Transformer [61]	86.6	83.7	7.8
PointMLP [28]	86.1	84.6	-
Stratifiedformer [17]	86.6	85.1	-
PointNet++ [33]	85.1	81.9	1.0
PointNeXt-S \dagger [35]	86.7 \pm 0.0	84.4 \pm 0.2	1.0
PointNeXt-S \dagger [35] (C=64)	86.9 \pm 0.1	84.8 \pm 0.5	3.7
PointNeXt-S (C=160) [35]	86.5 \pm 0.1	-	22.5
PointNeXt-S \dagger (C=160) [35]	87.0 \pm 0.1	85.2 \pm 0.1	22.5
PointMamba [22]	86.0	84.4	17.4
PCM-Tiny (ours)	86.9	85.0	8.8
PCM-Tiny \dagger (ours)	87.1	85.3	8.8
PCM (ours)	87.0 \pm 0.2	85.3 \pm 0.1	40.6
PCM \dagger (ours)	87.1\pm0.2	85.6\pm0.1	40.6

the SOTA method PointNeXt by 0.4 in OA and 0.8 in mAcc. Compared to PointMLP, Mamba layers demonstrated significantly stronger modeling capabilities than MLP, with PointNeXt surpassing PointMLP by 2.7 in OA and 2.7 in mAcc. By reducing the number of Mamba layers and channel size, PCM-Tiny achieved an OA of 86.9 and a mAcc of 85.0 with only 20% of the parameters of PCM. It is worth noting that PCM-Tiny, with only 52% of the parameters of PointMLP (6.9 M vs. 13.2 M), still outperformed PointMLP by 1.5 in OA and 1.1 in mAcc.

3D object classification in ModelNet40 dataset. ModelNet40 [50] is a widely used synthetic 3D object classification dataset consisting of 40 categories, each with 100 unique CAD models. As shown in Table 2, PCM achieved an OA of 93.4 and a mAcc of 90.7, reaching a performance comparable to PointNeXt [35]. PCM-Tiny achieved an OA of 93.1 and a mAcc of 90.6 with approximately 20% of the parameters of PCM. However, due to the smaller scale and less challenging nature of ModelNet40, performance on this dataset is difficult to differentiate between different methods’ modeling capabilities significantly, with most methods’ OA concentrated between 93 and 94. It is worth noting that we replicated the experiments of PointMLP [28] but obtained an OA of 93.6, indicating that the high accuracy 94.1 requires multiple repetitions and selection of the best.

3D object part segmentation in ShapeNetPart dataset. ShapeNetPart [3] is a widely used dataset for 3D object part segmentation. It comprises 16,880 models from 16 different shape categories and 50 part labels. Experimental results on the ShapeNetPart dataset are shown in Table 3. PCM achieves 87.0 Ins. mIoU and 85.3 Cls. mIoU without using any test augmentation strategies such as voting, surpassing PointNeXt [35] by 0.5 Ins. mIoU. With the use of voting, PCM achieves 87.1 Ins. mIoU and 85.6 Cls. mIoU, surpassing PointNeXt by 0.1 mIoU and 0.4 Cls. mIoU. Point-Tiny, with only 8.8 M parameters, achieves 86.9 Ins. mIoU and 85.0 Cls. mIoU, surpassing PointNeXt with 22.5 M parameters by 0.4 Ins. mIoU. PCM outperforms PointMLP [28] by 1.0 Ins. mIoU and 1.0 Cls. mIoU, demonstrating the significant potential of Mamba for 3D point cloud modeling.

4.3 Ablation Analysis and Visualization

Serialization strategies. The key to applying Mamba for point cloud modeling is transforming point clouds into point sequences. As shown in Table 4, we conduct the ablation experiment with different serialization strategies. Similar performance is achieved when all Mamba layers’ inputs are serialized using a single order, whether it’s z-order, Hilbert-order, or our proposed xyz-order. However, significant performance gains are observed when more serialization strategies are employed. When the three variants of our proposed consistent traverse serialization, namely “xyz”, “yzx”, and

Table 4: **Ablation studies on serialization strategies.** Each mamba layer is assigned a serialization order and listed inside $\{ \}$. "xyz", "xzy", "yxz", "yzx", "zxy", and "zyx" represent different variants of our proposed Consistent Traverse Serialization.

Strategy	OA (%)	mAcc (%)
$\{ "z" \} \times 9$	86.78	84.67
$\{ "hilbert" \} \times 9$	86.78	84.68
$\{ "xyz" \} \times 9$	86.71	85.00
$\{ "xyz", "yzx", "zxy" \} \times 3$	86.88	85.11
$\{ "xyz", "xzy", "yxz", "yzx", "zxy", "xyz", "yzx", "zxy" \}$	87.10	85.51
$\{ "xyz", "xzy", "yxz", "yzx", "zxy", "xyz", "hilbert", "z", "z-trans" \}$	87.20	85.54

Table 5: **Ablation studies on channel size.** The four-stage feature channel sizes are listed inside $\{ \}$ and connected with $-$.

Channels	OA (%)	mAcc (%)	Params. (M)
$\{ 96-96-96-96 \}$	84.84	82.11	1.2
$\{ 192-192-192-192 \}$	85.91	84.35	3.7
$\{ 384-384-384-384 \}$	86.40	84.48	12.7
$\{ 768-768-768-768 \}$	87.52	85.87	47.2
$\{ 96-192-384-768 \}$	86.16	83.67	22.6
$\{ 384-384-768-768 \}$	87.40	85.52	34.2

Table 6: **Ablation on positional embedding.** "Share" refers to learning a mapping function for all Mamba layers with the same channel size.

Type	Share	OA (%)	mAcc (%)
RoPE	-	86.95	85.09
Learnable Embedding	-	87.01	85.56
Linear	✓	87.32	85.89
MLP	✓	87.26	85.82
Linear	✗	87.10	85.78
MLP	✗	87.12	85.79

"zxy", are used together, PCM demonstrates a performance improvement of 0.17 OA and 0.11 mAcc compared to using only the "xyz" variant. When all six variants of consistent traverse serialization are combined, PCM shows a performance improvement of 0.39 OA and 0.51 mAcc. When all six variants of consistent traverse serialization, as well as "Hilbert," "z," and "z-trans" serialization strategies, are combined, PCM achieves a performance improvement of 0.49 OA and 0.54 mAcc. Different serialization strategies allow different Mamba layers to observe point clouds from different perspectives, resulting in more robust modeling of point cloud features.

Channel size. When the SSM-based method processes a token in the sequence, it relies solely on the hidden states and the input token, so the hidden states must have sufficient channel size to store global information. To investigate this, we conducted ablation studies on channel size, and the results are shown in Table 5. When the channel size is reduced from 768 to 384, PCM exhibits a performance decay of 1.12 OA and 1.41 mAcc. A significant performance decay of 2.56 OA and 3.76 mAcc is observed when the channel size is reduced to 96. We then attempted to reduce the channel size of early stages, and the results show that excessively reducing the channel size of early stages (from 768 to 96) still leads to a performance decay of 1.36 OA and 2.2 mAcc. However, moderately reducing the channel size of the first two stages (from 768 to 384) only results in minor performance decay but can save significant computation. Therefore, in our final configuration, the first two stages adopt a channel size 384, while the last two stages use a channel size 768.

Positional embedding. We evaluate the impact of different positional encoding strategies, and the results are shown in Table 6. Initially, we experimented with rotary position embedding; however, it yielded the poorest performance. This is attributed to RoPE encoding solely the sequence order, unsuited for sparse and irregular point cloud data. Learnable positional embedding, a common practice in image sequence modeling, similarly encodes the sequence position and performs comparably to rotary positional encoding. Achieving favorable outcomes can be as straightforward as mapping point cloud spatial coordinates using a Linear layer as the positional encoding, resulting in a performance improvement of 0.37 OA and 0.7 mAcc compared to RoPE. Replacing the linear layer with a stronger MLP did not enhance performance. Nevertheless, the performance deteriorated due to overfitting when employing a separate Linear layer for each mamba layer.

Order prompts. To enhance the understanding of point cloud sequences by Mamba layers, we propose order prompts and conduct ablation experiments to validate their effectiveness, as shown in Table 7. When using only one order prompt, PCM demonstrates a performance improvement of 0.38 OA and 0.73 mAcc compared to not using any order prompt. Performance peaks when using six order prompts, resulting in a performance gain of 0.83 OA and 1.47 mAcc compared to no order

Table 7: **Ablation on numbers of order prompts.**

Prompts	OA (%)	mAcc (%)
0	86.64	84.70
1	87.02	85.43
3	86.88	84.78
6	87.47	86.17
12	87.13	85.28

Table 8: **Ablation on neighborhood points.**

K	Stride	OA (%)	mAcc (%)
0	-	79.32	76.25
4	1	84.66	82.72
8	1	86.95	85.06
12	1	87.37	85.96
24	1	87.09	85.10
24	2	85.39	83.55

Table 9: **Ablation on points downsampling.** The number of points at different stages is listed within {} and connected with -.

Points	OA (%)	mAcc (%)
{1024-1024-1024-1024}	87.35	85.71
{1024-512-256-128}	87.20	85.54
{512-256-128-128}	86.95	85.32
{512-256-128-64}	86.68	85.12

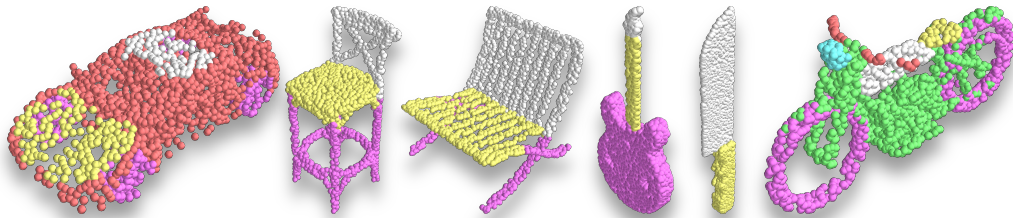


Figure 5: **The visualization results of part segmentation on the ShapeNetPart dataset.**

prompt. However, further increasing the number of order prompts does not yield higher performance gains, although it still significantly outperforms not using any order prompt.

Local features. 3D point cloud data are sparse and have low semantic density, making local features crucial for understanding point clouds. We conducted ablation experiments on computing local features using different numbers of neighboring points, and the results are shown in Table 8. When the number of neighboring points is set to 0, meaning no local features are computed, and only relying on Mamba layers to model the global features of the point cloud, PCM achieves an OA of 79.32 and a mAcc of 76.25. Using only four neighboring points to compute local features, PCM improves performance with an OA of 84.66 and a mAcc of 82.72, showing an increase of 5.34 OA and 6.47 mAcc compared to when local features are not used. PCM achieves the highest performance when using 12 points for computing local features. However, with a further increase in the number of neighboring points, performance decreases, indicating that the current local feature extraction mechanism, such as the geometric affine module in PointMLP, is not proficient at modeling the global features of point clouds. Therefore, combining local feature extraction modules and Mamba layers to model point clouds' local and global features is a promising approach.

Point downsampling. Point cloud data exhibit significant redundancy; thus, appropriate point downsampling can substantially reduce computational costs with minimal loss in performance. We experimented with several downsampling schemes, and the results are shown in Table 9. Down-sampling by a factor of 2 for all stages except the first stage resulted in only a slight performance decrease of 0.15 OA and 0.17 mAcc while significantly reducing computation. However, excessive downsampling, leaving only 64 points for the last stage, led to a performance drop of 0.67 OA and 0.59 mAcc. We ultimately adopted a downsampling strategy of line 2 for PCM.

5 Conclusion

This paper introduces a Mamba-based point cloud network named Point Cloud Mamba, which, for the first time, beats the SOTA point-based method PointNeXt. Point Cloud Mamba incorporates several novel techniques to assist Mamba in better modeling point cloud data. Firstly, we propose Consistent Traverse Serialization to convert 3D point cloud data into 1D point sequences that Mamba can handle, ensuring that neighbouring points in the sequence are also spatially adjacent. Secondly, we aid Mamba in handling point sequences serialized in different orders by introducing order prompts containing sequence arrangement rules. Finally, we propose a simple yet effective positional encoding based on spatial coordinate mapping. Point Cloud Mamba achieves SOTA performance on the ScanObjectNN, ModelNet40, and ShapeNetPart datasets.

References

- [1] Ali Behrouz and Farnoosh Hashemi. Graph Mamba: Towards Learning on Graphs with State Space Models. 2024. 3
- [2] Nicolas Carion, Francisco Massa, Gabriel Synnaeve, Nicolas Usunier, Alexander Kirillov, and Sergey Zagoruyko. End-to-end object detection with transformers. In *ECCV*, 2020. 3
- [3] Angel X Chang, Thomas Funkhouser, Leonidas Guibas, Pat Hanrahan, Qixing Huang, Zimo Li, Silvio Savarese, Manolis Savva, Shuran Song, Hao Su, et al. Shapenet: An information-rich 3d model repository. *arXiv:1512.03012*, 2015. 7, 8
- [4] Guangyan Chen, Meiling Wang, Yi Yang, Kai Yu, Li Yuan, and Yufeng Yue. Pointgpt: Auto-regressively generative pre-training from point clouds. *arXiv:2305.11487*, 2023. 2
- [5] Alexey Dosovitskiy, Lucas Beyer, Alexander Kolesnikov, Dirk Weissenborn, Xiaohua Zhai, Thomas Unterthiner, Mostafa Dehghani, Matthias Minderer, Georg Heigold, Sylvain Gelly, et al. An image is worth 16x16 words: Transformers for image recognition at scale. In *ICLR*, 2021. 3
- [6] Zhongbin Fang, Xiangtai Li, Xia Li, Joachim M Buhmann, Chen Change Loy, and Mengyuan Liu. Explore in-context learning for 3d point cloud understanding. *NeurIPS*, 2023. 2
- [7] Ankit Goyal, Hei Law, Bowei Liu, Alejandro Newell, and Jia Deng. Revisiting point cloud shape classification with a simple and effective baseline. In *ICML*, 2021. 7
- [8] Albert Gu and Tri Dao. Mamba: Linear-time sequence modeling with selective state spaces. *arXiv preprint arXiv:2312.00752*, 2023. 2, 3, 4
- [9] Albert Gu, Karan Goel, and Christopher Ré. Efficiently modeling long sequences with structured state spaces. *arXiv preprint arXiv:2111.00396*, 2021. 4
- [10] Albert Gu, Karan Goel, and Christopher Ré. Efficiently modeling long sequences with structured state spaces. In *ICLR*, 2022. 2, 3
- [11] Meng-Hao Guo, Jun-Xiong Cai, Zheng-Ning Liu, Tai-Jiang Mu, Ralph R Martin, and Shi-Min Hu. Pct: Point cloud transformer. In *CVM*, 2021. 3, 7
- [12] Xuanhua He, Ke Cao, Keyu Yan, Rui Li, Chengjun Xie, Jie Zhang, and Man Zhou. Pan-mamba: Effective pan-sharpening with state space model. *arXiv preprint arXiv:2402.12192*, 2024. 3
- [13] David Hilbert and David Hilbert. Über die stetige abbildung einer linie auf ein flächenstück. *Dritter Band: Analysis· Grundlagen der Mathematik· Physik Verschiedenes: Nebst Einer Lebensgeschichte*, pages 1–2, 1935. 5
- [14] Jincen Jiang, Xuequan Lu, Lizhi Zhao, Richard Dazeley, and Meili Wang. Masked autoencoders in 3d point cloud representation learning. *arXiv:2207.01545*, 2022. 2
- [15] Artem Komarichev, Zichun Zhong, and Jing Hua. A-cnn: Annularly convolutional neural networks on point clouds. In *CVPR*, 2019. 2
- [16] Jean Lahoud, Jiale Cao, Fahad Shahbaz Khan, Hisham Cholakkal, Rao Muhammad Anwer, Salman Khan, and Ming-Hsuan Yang. 3d vision with transformers: A survey, 2022. 3
- [17] Xin Lai, Jianhui Liu, Li Jiang, Liwei Wang, Hengshuang Zhao, Shu Liu, Xiaojuan Qi, and Jiaya Jia. Stratified transformer for 3d point cloud segmentation. In *CVPR*, 2022. 3, 8
- [18] Guohao Li, Matthias Müller, Guocheng Qian, Itzel Carolina Delgadillo Perez, Abdulellah Abualshour, Ali Kassem Thabet, and Bernard Ghanem. Deepgcns: Making gcns go as deep as cnns. *PAMI*, 2021. 7
- [19] Shufan Li, Harkanwar Singh, and Aditya Grover. Mamba-nd: Selective state space modeling for multi-dimensional data. *arXiv preprint arXiv:2402.05892*, 2024. 3
- [20] Xiangtai Li, Henghui Ding, Wenwei Zhang, Haobo Yuan, Guangliang Cheng, Pang Jiangmiao, Kai Chen, Ziwei Liu, and Chen Change Loy. Transformer-based visual segmentation: A survey. *arXiv pre-print*, 2023. 3
- [21] Yangyan Li, Rui Bu, Mingchao Sun, Wei Wu, Xinhan Di, and Baoquan Chen. Pointcnn: Convolution on x-transformed points. In *NeurIPS*, 2018. 2, 7
- [22] Dingkang Liang, Xin Zhou, Xinyu Wang, Xingkui Zhu, Wei Xu, Zhikang Zou, Xiaoqing Ye, and Xiang Bai. Pointmamba: A simple state space model for point cloud analysis. *arXiv preprint arXiv:2402.10739*, 2024. 2, 7, 8
- [23] Haotian Liu, Mu Cai, and Yong Jae Lee. Masked discrimination for self-supervised learning on point clouds. In *ECCV*, 2022. 2
- [24] Yongcheng Liu, Bin Fan, Shiming Xiang, and Chunhong Pan. Relation-shape convolutional neural network for point cloud analysis. In *CVPR*, 2019. 2
- [25] Yue Liu, Yunjie Tian, Yuzhong Zhao, Hongtian Yu, Lingxi Xie, Yaowei Wang, Qixiang Ye, and Yunfan Liu. Vmamba: Visual state space model. *arXiv preprint arXiv:2401.10166*, 2024. 3, 5
- [26] Ilya Loshchilov and Frank Hutter. Decoupled weight decay regularization. *arXiv preprint arXiv:1711.05101*, 2017. 7
- [27] Jun Ma, Feifei Li, and Bo Wang. U-mamba: Enhancing long-range dependency for biomedical image segmentation. *arXiv preprint arXiv:2401.04722*, 2024. 3
- [28] Xu Ma, Can Qin, Haoxuan You, Haoxi Ran, and Yun Fu. Rethinking network design and local geometry in point cloud: A simple residual mlp framework. In *ICLR*, 2022. 1, 2, 3, 4, 7, 8

[29] Guy M Morton. A computer oriented geodetic data base and a new technique in file sequencing. 1966. 4, 5

[30] Yatian Pang, Wenxiao Wang, Francis EH Tay, Wei Liu, Yonghong Tian, and Li Yuan. Masked autoencoders for point cloud self-supervised learning. In *ECCV*, 2022. 1, 7

[31] Yatian Pang, Wenxiao Wang, Francis EH Tay, Wei Liu, Yonghong Tian, and Li Yuan. Masked autoencoders for point cloud self-supervised learning. In *ECCV*, 2022. 2

[32] Charles R Qi, Hao Su, Kaichun Mo, and Leonidas J Guibas. Pointnet: Deep learning on point sets for 3d classification and segmentation. In *CVPR*, 2017. 1, 2, 7, 8

[33] Charles Ruizhongtai Qi, Li Yi, Hao Su, and Leonidas J Guibas. Pointnet++: Deep hierarchical feature learning on point sets in a metric space. In *NeurIPS*, 2017. 1, 2, 7, 8

[34] Guocheng Qian, Hasan Hammoud, Guohao Li, Ali Thabet, and Bernard Ghanem. Assanet: An anisotropical separable set abstraction for efficient point cloud representation learning. In *NeurIPS*, 2021. 7, 8

[35] Guocheng Qian, Yuchen Li, Houwen Peng, Jinjie Mai, Hasan Hammoud, Mohamed Elhoseiny, and Bernard Ghanem. Pointnext: Revisiting pointnet++ with improved training and scaling strategies. *NeurIPS*, 2022. 1, 2, 5, 7, 8

[36] Haoxi Ran, Jun Liu, and Chengjie Wang. Surface representation for point clouds. In *CVPR*, 2022. 2

[37] Jiacheng Ruan and Suncheng Xiang. Vm-unet: Vision mamba unet for medical image segmentation. *arXiv preprint arXiv:2402.02491*, 2024. 3

[38] Jonas Schult, Francis Engelmann, Alexander Hermans, Or Litany, Siyu Tang, and Bastian Leibe. Mask3D: Mask Transformer for 3D Semantic Instance Segmentation. 2023. 3

[39] Yiru Shen, Chen Feng, Yaoqing Yang, and Dong Tian. Mining point cloud local structures by kernel correlation and graph pooling. In *CVPR*, 2018. 2

[40] Jianlin Su, Murtadha Ahmed, Yu Lu, Shengfeng Pan, Wen Bo, and Yunfeng Liu. Roformer: Enhanced transformer with rotary position embedding. *Neurocomputing*, 568:127063, 2024. 2, 6

[41] Jiahao Sun, Chunmei Qing, Junpeng Tan, and Xiangmin Xu. Superpoint transformer for 3d scene instance segmentation. *AAAI*, 2023. 3

[42] Hugues Thomas, Charles R Qi, Jean-Emmanuel Deschaud, Beatriz Marcotegui, François Goulette, and Leonidas J Guibas. Kpconv: Flexible and deformable convolution for point clouds. In *ICCV*, 2019. 2, 7, 8

[43] Mikaela Angelina Uy, Quang-Hieu Pham, Binh-Son Hua, Thanh Nguyen, and Sai-Kit Yeung. Revisiting point cloud classification: A new benchmark dataset and classification model on real-world data. In *ICCV*, 2019. 2, 7

[44] Ashish Vaswani, Noam Shazeer, Niki Parmar, Jakob Uszkoreit, Llion Jones, Aidan N Gomez, Łukasz Kaiser, and Illia Polosukhin. Attention is all you need. In *NeurIPS*, 2017. 2

[45] Xinshun Wang, Zhongbin Fang, Xia Li, Xiangtai Li, Chen Chen, and Mengyuan Liu. Skeleton-in-context: Unified skeleton sequence modeling with in-context learning. *CVPR*, 2024. 2

[46] Yue Wang, Yongbin Sun, Ziwei Liu, Sanjay E Sarma, Michael M Bronstein, and Justin M Solomon. Dynamic graph cnn for learning on point clouds. In *TOG*, 2019. 7, 8

[47] Wenzuan Wu, Zhongang Qi, and Li Fuxin. Pointconv: Deep convolutional networks on 3d point clouds. In *CVPR*, 2019. 2

[48] Xiaoyang Wu, Li Jiang, Peng-Shuai Wang, Zhijian Liu, Xihui Liu, Yu Qiao, Wanli Ouyang, Tong He, and Hengshuang Zhao. Point transformer v3: Simpler, faster, stronger. In *CVPR*, 2024. 3

[49] Xiaoyang Wu, Yixing Lao, Li Jiang, Xihui Liu, and Hengshuang Zhao. Point transformer v2: Grouped vector attention and partition-based pooling. In *NeurIPS*, 2022. 3

[50] Zhirong Wu, Shuran Song, Aditya Khosla, Fisher Yu, Linguang Zhang, Xiaoou Tang, and Jianxiong Xiao. 3d shapenets: A deep representation for volumetric shapes. In *CVPR*, 2015. 2, 7, 8

[51] Tiange Xiang, Chaoyi Zhang, Yang Song, Jianhui Yu, and Weidong Cai. Walk in the cloud: Learning curves for point clouds shape analysis. In *ICCV*, 2021. 2

[52] Tiange Xiang, Chaoyi Zhang, Yang Song, Jianhui Yu, and Weidong Cai. Walk in the cloud: Learning curves for point clouds shape analysis. In *ICCV*, 2021. 7, 8

[53] Saining Xie, Jiatao Gu, Demi Guo, Charles R Qi, Leonidas Guibas, and Or Litany. Pointcontrast: Unsupervised pre-training for 3d point cloud understanding. In *ECCV*, 2020. 2

[54] Zhaohu Xing, Tian Ye, Yijun Yang, Guang Liu, and Lei Zhu. Segmamba: Long-range sequential modeling mamba for 3d medical image segmentation. *arXiv preprint arXiv:2401.13560*, 2024. 3

[55] Mutian Xu, Runyu Ding, Hengshuang Zhao, and Xiaojuan Qi. Paconv: Position adaptive convolution with dynamic kernel assembling on point clouds. In *CVPR*, 2021. 2

[56] Mutian Xu, Junhao Zhang, Zhipeng Zhou, Mingye Xu, Xiaojuan Qi, and Yu Qiao. Learning geometry-disentangled representation for complementary understanding of 3d object point cloud. In *AAAI*, 2021. 2

[57] Yijun Yang, Zhaohu Xing, and Lei Zhu. Vivim: a video vision mamba for medical video object segmentation. *arXiv preprint arXiv:2401.14168*, 2024. 3

[58] Li Yi, Vladimir G Kim, Duygu Ceylan, I-Chao Shen, Mengyan Yan, Hao Su, Cewu Lu, Qixing Huang, Alla Sheffer, and Leonidas Guibas. A scalable active framework for region annotation in 3d shape collections. In *TOG*, 2016. 2

- [59] Xumin Yu, Lulu Tang, Yongming Rao, Tiejun Huang, Jie Zhou, and Jiwen Lu. Point-bert: Pre-training 3d point cloud transformers with masked point modeling. In *CVPR*, 2022. [2](#), [7](#)
- [60] Zaiwei Zhang, Rohit Girdhar, Armand Joulin, and Ishan Misra. Self-supervised pretraining of 3d features on any point-cloud. In *ICCV*, 2021. [2](#)
- [61] Hengshuang Zhao, Li Jiang, Jiaya Jia, Philip H.S. Torr, and Vladlen Koltun. Point transformer. In *ICCV*, 2021. [1](#), [3](#), [8](#)
- [62] Lianghui Zhu, Bencheng Liao, Qian Zhang, Xinlong Wang, Wenyu Liu, and Xinggang Wang. Vision mamba: Efficient visual representation learning with bidirectional state space model. *arXiv preprint arXiv:2401.09417*, 2024. [3](#), [5](#)